Bis-(imidazole/benzimidazole)-pyridine derivatives: synthesis, structure and antimycobacterial activity

Vasilichia Antoci[1], Dumitrela Cucu[1], Gheorghita Zbancioc[1], Costel Moldoveanu[1], Violeta Mangalagiu*,[2], Dorina Amariucai-Mantu[1], Aculina Aricu[3] & Ionel I Mangalagiu**,[1,2] (iD)

[1]Faculty of Chemistry, Alexandru Ioan Cuza University of Iasi, 11 Carol I Bd, Iasi 700506, Romania
[2]Interdisciplinary Research Institute – CERNESIM Center, Alexandru Ioan Cuza University of Iasi, 11 Carol I Bd, Iasi 700506, Romania
[3]Institute of Chemistry, Academiei Street 3, 2028 Chisinau, Moldova
*Author for correspondence: violetaren@yahoo.com
**Author for correspondence: ionelm@uaic.ro

Aim: Over the last decades, few significant achievements have been made in tuberculosis (TB) therapy. As a result, there is an urgent need for new anti-TB drugs. **Results:** Two new classes of *bis*-(imidazole/benzimidazole)-pyridine derivatives were designed, synthesized and evaluated for their antimycobacterial activity. **Conclusion:** The synthesis is efficient and straightforward, involving only two successive *N*-alkylations. The anti-TB assay reveal that our compounds have an excellent anti-TB activity against both replicating and nonreplicating *Mtb*, are not cytotoxic, exhibited a very good intracellular activity and are active against drug-resistant *Mtb* strains, some compounds have a bactericidal mechanism. The absorption, distribution, metabolism, excretion and toxicity studies performed for one compound are promising, indicating that it is a good candidate for a future drug.

During the last two centuries, tuberculosis (TB) became an extremely aggressive disease responsible for millions of deaths around the world [1]. According to the WHO, TB now remains a leading infectious disease worldwide, almost a third of the world's population (around 2 billion people) being infected with nonreplicating *Mtb* [1]. Drug-resistant TB, multidrug-resistant TB, extensively drug-resistant TB and totally drug-resistant TB are present in almost all countries all around the world, and making the situation even more challenging for global TB treatment. In 2017, there were around 700,000 new cases with resistance to rifampicin, the most effective first-line drug, of which 500,000 had multi-drug resistant-TB [1–3]. In addition, association of TB with HIV/AIDS complicates the situation for patients even more, with TB being the leading cause of death among the patients infected with HIV (in 2017, there were an estimated 400,000 TB deaths among HIV-positive people) [1,4,5]. As a result of these considerations, each year (in the last 5), there were an estimated two million TB deaths and about eight million new cases of TB reported [1].

The TB treatment is a challenging, complex and extremely difficult task. In the last 50 years, only two new drugs (bedaquiline [6] and delamanid [7]) have been developed in anti-TB therapies, for drug-resistant strains of *Mtb*. Therefore, the search for new anti-TB drugs active against *Mtb* remains one of the priority tasks of medicinal chemistry. There are currently several strategies used for the development of new anti-TB drugs [8–11], one of the most important and used strategy consist of searching for novel structures which the TB organism has never encountered with before. Nitrogen heterocyclic compounds, especially five and six member ring derivatives, represent the most effective and administered class of drugs in TB therapy. Among them, pyridine and imidazole/benzimidazole derivatives play a central role, the most effective and promising anti-TB drugs being related to these classes [8–18].

Encouraged by the above considerations and in continuation of our research in the area of new antimycobacterial compounds with azaheterocyclic skeleton [18–30], we report herein the design, synthesis and antimycobacterial activity of a new class of *bis*-(imidazole/benzimidazole)-pyridine (BIP) derivatives.

Experimental

Materials & measurements

Melting points were determined using an electrothermal Mel-Temp apparatus and were uncorrected (Barnstead International, IA, USA). The nuclear magnetic experiments (^{1}H-NMR, ^{13}C-NMR, 2D-COSY, 2D-HMQC, 2D-HMBC) were recorded using Bruker Avance III 500/Bruker Avance DRX 400 spectrometers (Bruker, Vienna, Austria) operating at 500/400 and 125/100 MHz for ^{1}H and, respectively, ^{13}C nuclei. The following abbreviations were used to designate chemical shift multiplicities: s = singlet, d = doublet, t = triplet, m = multiplet, brs = broad singlet, ad = apparent doublet, at = apparent triplet. All chemical shifts are reported in δ units (p.p.m.) relative to the residual peak of solvent (ref: DMSO, [1]H: 2.50 p.p.m.; [13]C: 39.52 p.p.m.). Coupling constants (*J*) are given in Hz. The IR spectra were recorded on a Fourier transform IR (FTIR) Shimadzu Prestige 8400s spectrophotometer (Shimadzu, Kyoto, Japan). Thin layer chromatography (TLC) was carried out on Merck silica gel 60F$_{254}$ plates. Visualization of the plates was achieved using a UV lamp (λ_{max} = 254 or 365 nm). The ultrasonic bath Elma Transsonic T310 (power 34.5 W, frequency 35 kHz; Elma Schmidtbauer, Singen, Germany) was used for solubilizing the starting materials. The micro-analyses were in satisfactory agreement with the calculated values: C, $\pm$ 0.15; H, $\pm$ 0.10; N, $\pm$ 0.30.

Compounds **2a** and **5** were previously reported [31].

General procedure for synthesis of starting materials 2a,b & 5

To a solution of imidazole/4-nitroimidazole (3 mmol, 3 equivalent, 0.20 g/0.34 g, dissolved in 15 ml tetrahydrofuran dry/35 ml dimethylformamide using US bath), or benzimidazole (2.4 mmol, 2.4 equivalent, 0.28 g, dissolved in 15 tetrahydrofuran dry), was added dropwise, at 0°C (ice), NaH (60% in mineral oil; 3.6 mmol, 3.6 equivalent, 0.14 g, suspended in 15 ml tetrahydrofuran dry). The sodium hydride was firstly washed three times with 5 ml *n*-hexane. Then, 2,6-*bis*(halogenomethyl)pyridine **1** (1 mmol, 1 equivalent, 0.18 g (X = -Cl for the solution of imidazole/4-nitroimidazole), 0.26 g (X = -Br for the solution of benzimidazole) dissolved in 15 ml tetrahydrofuran dry), was added dropwise. The resulting solutions were stirred for additional time (72, 24, 96 h) at room temperature, to give the corresponding starting materials **2a,b** and **5**. The solutions were filtered off, concentrated on rotary evaporator, than precipitated with diethyl ether for compounds **2a** and **5**, or dimethylformamide/methanol: 3/15 (v/v), for compound **2b**. The formed precipitates were collected by filtration and dried *in vacuo*.

General procedure for synthesis of quaternary salts 4a–g

A solution of 2,6-*bis*((1*H*-imidazol-1-*yl*)methyl)pyridine **2a** (1 mmol, 1 equivalent, 0.24 g, dissolved in 40 ml acetone using the ultrasound bath) and the α-halogeno ester and amide (2.4 mmol, 2.4 equivalent, 0.22 ml **3a**, 0.44 g **3b**) or the bromacetophenone derivatives (2.8 mmol, 2.8 equivalent, 0.56 g **3c**, 0.78 g **3d**, 0.65 g **3e**, 0.68 g **3f**, 0.64 g **3g**) solubilized in acetone (15 ml), was magnetically stirred for 24 h, to give the corresponding quaternary salts **4a–g**. The completion of the reactions was carried out using TLC. The obtained salts were filtered off, washed two times with the same solvent (10 ml) and dried *in vacuo*. No other purification required.

General procedure for synthesis of quaternary salts 6a–g

To a solution of 2,6-*bis*((1*H*-benzo[*d*]imidazol-1-*yl*)methyl)pyridine **5** (1 mmol, 1 equivalent, 0.34 g, dissolved in 40 ml acetone using the ultrasound bath) were added the α-halogeno ester and amide (4.8 mmol, 4.8 equivalent, 0.73 ml **3a**, 0.89 g **3b**) or the bromacetophenone derivatives (4.5 mmol, 4.5 equivalent, 0.89 g **3c**, 1.25 g **3d**, 1.05 g **3e**, 1.1 g **3f**, 1.03 g **3g**) solubilized in acetone (20 ml). The solutions were refluxed for 12 h and magnetically stirred for another 12 h, resulting the desired salts **6a–g**. TLC was used for follow the evolution of chemical reactions. The precipitates were collected by filtration, then washed with acetone (3 times with 10 ml) and dried in vacuum. No other purification required.

Spectral data of starting materials 2a,b & 5
2,6-bis((1H-imidazol-1-yl)methyl)pyridine (2a)

Appearance: white powder. Yield, 76%. melting point (mp) 98–106°C. FTIR (KBr) cm^{-1} = 3101, 2987, 1595, 1506, 1431, 1230. ^{1}H-NMR (400 MHz, DMSO-*d6*) δ = 7.81–7.77 (t, *J* = 7.6 Hz, 1H, H$_4$), 7.75 (s, 2H, 2xH$_{2'}$), 7.20 (s, 2H, 2xH$_{5'}$), 7.05–7.03 (d, *J* = 7.6 Hz, 2H, 2xH$_3$), 6.93 (s, 2H, 2xH$_{4'}$), 5.30 (s, 4H, 2xCH$_2$). ^{13}C-NMR (100 MHz, DMSO-*d6*) δ = 156.7 2xC$_2$, 138.5 C$_4$, 137.7 2xC$_{2'}$, 128.6 2xC$_{4'}$, 120.3 2xC$_3$, 119.8 2xC$_{5'}$, 51.1 2xCH$_2$. Anal. Calcd. for C$_{13}$H$_{13}$N$_5$: C, 65.25; H, 5.48; N, 29.27; found: C, 65.40; H, 5.38; N, 29.57.

2,6-bis((4-nitro-1H-imidazol-1-yl)methyl)pyridine (2b)

Appearance: white powder. Yield, 72%. mp 189–195°C. FTIR (KBr) cm^{-1} = 3140, 3119, 1595, 1525, 1485, 1330. ^{1}H-NMR (400 MHz, DMSO-*d6*) δ = 8.36 (ad, 2H, 2xH$_{2'}$), 7.91–7.87 (at, *J* = 8.0 Hz, 3H, 2xH$_{5'}$, H$_4$), 7.34–7.32 (d, *J* = 7.6 Hz, 2H, 2xH$_3$), 5.42 (s, 4H, 2xCH$_2$). ^{13}C-NMR (100 MHz, DMSO-*d6*) δ = 154.9 2xC$_2$, 146.9 2xC$_{4'}$, 138.7 C$_4$, 137.7 2xC$_{5'}$, 121.8 2xC$_{2'}$, 121.2 2xC$_3$, 51.6 2xCH$_2$. Anal. Calcd. for C$_{13}$H$_{11}$N$_7$O$_4$: C, 47.42; H, 3.37; N, 29.78; found: C, 47.32; H, 3.30; N, 29.98.

2,6-bis((1H-benzo[d]imidazol-1-yl)methyl)pyridine (5)

Appearance: white powder. Yield, 64%. mp 154–160°C. FTIR (KBr) cm^{-1} = 3120, 2990, 1590, 1526, 1451, 1270. ^{1}H-NMR (500 MHz, DMSO-*d6*) δ = 8.35 (s, 2H, 2xH$_{2'}$), 7.74–7.71 (t, *J* = 8.0 Hz, 1H, H$_4$), 7.66–7.65 (d, *J* = 8.0 Hz, 2H, 2xH$_{7'}$), 7.40–7.38 (d, *J* = 8.0 Hz, 2H, 2xH$_{4'}$), 7.19–7.11 (m, 6H, 2xH$_{6'}$, 2xH$_3$, 2xH$_{5'}$), 5.54 (s, 4H, 2xCH$_2$). ^{13}C- NMR (125 MHz, DMSO-*d6*) δ = 155.9 2xC$_2$, 144.4 2xC$_{2'}$, 143.4 2xC$_{3'a}$, 138.4 C$_4$, 133.7 2xC$_{7'a}$, 122.4 2xC$_{5'}$, 121.5 2xC$_{6'}$, 120.9 2xC$_3$, 119.4 2xC$_{7'}$, 110.6 2xC$_{4'}$, 49.4 2xCH$_2$. Anal. Calcd. for C$_{21}$H$_{17}$N$_5$: C, 74.32; H, 5.05; N, 20.63; found: C, 74.47; H, 5.15; N, 20.33.

Spectral data of quaternary salts 4a–g & 6a–g
1,1′-(pyridine-2,6-diylbis(methylene))bis(3-(2-methoxy-2-oxoethyl)-1H-imidazol-3-ium) bromide (4a)

Appearance: white powder. Yield, 50%. mp 83–85°C. FTIR (KBr) cm^{-1} = 3095, 2983, 1730, 1593, 1440, 1240, 1070. ^{1}H-NMR (500 MHz, DMSO-*d6*) δ = 9.33 (s, 2H, 2xH$_{2'}$), 8.00–7.97 (t, *J* = 7.5 Hz, 1H, H$_4$), 7.80 (s, 2H, 2xH$_{4'}$), 7.75 (s, 2H, 2xH$_{5'}$), 7.53–7.52 (d, *J* = 8.0 Hz, 2H, 2xH$_3$), 5.67 (s, 4H, 2xCH$_2$-α), 5.39 (s, 4H, 2xCH$_2$-β), 3.76 (s, 6H, 2xCH$_3$). ^{13}C-NMR (125 MHz, DMSO-*d6*) δ = 167.4 2xCO, 153.4 2xC$_2$, 138.8 C$_4$, 137.8 2xC$_{2'}$, 123.6 2xC$_{4'}$, 123.0 2xC$_{5'}$, 122.2 2xC$_3$, 52.8 2xCH$_3$, 52.6 2xCH$_2$-α, 49.7 2xCH$_2$-β. Anal. Calcd. for C$_{19}$H$_{23}$Br$_2$N$_5$O$_4$: C, 41.85; H, 4.25; N, 12.84; found: C, 41.95; H, 4.34; N, 12.65.

1,1′-(pyridine-2,6-diylbis(methylene))bis(3-(2-amino-2-oxoethyl)-1H-imidazol-3-ium) iodide (4b)

Appearance: yellowish powder. Yield, 68%. mp 182–184°C. FTIR (KBr) cm^{-1} = 3348, 3140, 3079, 2940, 1679, 1584, 1520, 1432. ^{1}H-NMR (500 MHz, DMSO-*d6*) δ = 9.15 (s, 2H, 2xH$_{2'}$), 8.00–7.97 (t, *J* = 7.5 Hz, 1H, H$_4$), 7.88 (brs, 2H, 2x(-NH-)), 7.68 (s, 4H, 2xH$_{4'}$, 2xH$_{5'}$), 7.55 (brs, 2H, 2x(-NH-)), 7.51–7.49 (d, *J* = 7.5 Hz, 2H, 2xH$_3$), 5.59 (s, 4H, 2xCH$_2$-α), 5.01 (s, 4H, 2xCH$_2$-β). ^{13}C-NMR (125 MHz, DMSO-*d6*) δ = 166.7 2xCO, 153.5 2xC$_2$, 138.9 C$_4$, 137.8 2xC$_{2'}$, 123.8 2xC$_{4'}$, 122.5 2xC$_{5'}$, 122.1 2xC$_3$, 52.6 2xCH$_2$-α, 50.6 2xCH$_2$-β. Anal. Calcd. for C$_{17}$H$_{21}$I$_2$N$_7$O$_2$: C, 33.52; H, 3.47; N, 16.09; found: C, 33.67; H, 3.57; N, 15.84.

1,1′-(pyridine-2,6-diylbis(methylene))bis(3-(2-oxo-2-phenylethyl)-1H-imidazol-3-ium) bromide (4c)

Appearance: white powder. Yield, 85%. mp 165–167°C. FTIR (KBr) cm^{-1} = 3080, 2920, 1687, 1583, 1525, 1430. ^{1}H-NMR (500 MHz, DMSO-*d6*) δ = 9.30 (s, 2H, 2xH$_{2'}$), 8.06–8.01 (m, 5H, 4xH$_{2''}$, H$_4$), 7.82–7.81 (ad, 4H, 2xH$_{4'}$, 2xH$_{5'}$), 7.77–7.74 (t, *J* = 7.5 Hz, 2H, 2xH$_{4''}$), 7.62–7.57 (m, 6H, 4xH$_{3''}$, 2xH$_3$), 6.21 (s, 4H, 2xCH$_2$-β), 5.74 (s, 4H, 2xCH$_2$-α). ^{13}C-NMR (125 MHz, DMSO-*d6*) δ = 191.4 2xCO, 153.6 2xC$_2$, 138.8 C$_4$, 137.8 2xC$_{2'}$, 134.5 2xC$_{4''}$, 133.6 2xC$_{1''}$, 129.0 4xC$_{3''}$, 128.1 4xC$_{2''}$, 123.9 2xC$_{4'}$, 122.9 2xC$_{5'}$, 122.1 2xC$_3$, 55.6 2xCH$_2$-β, 52.6 2xCH$_2$-α. Anal. Calcd. for C$_{29}$H$_{27}$Br$_2$N$_5$O$_2$: C, 54.65; H, 4.27; N, 10.99; found: C, 54.55; H, 4.36; N, 10.79.

1,1′-(pyridine-2,6-diylbis(methylene))bis(3-(2-(4-bromophenyl)-2-oxoethyl)-1H-imidazol-3-ium) bromide (4d)

Appearance: white powder. Yield, 92%. mp 238–240°C. FTIR (KBr) cm^{-1} = 3115, 3070, 2960, 1695, 1583, 1560, 610. ^{1}H-NMR (500 MHz, DMSO-*d6*) δ = 9.26 (s, 2H, 2xH$_{2'}$), 8.04–8.01 (t, *J* = 8.0 Hz, 1H, H$_4$), 7.97–7.95 (d, *J* = 9.0 Hz, 4H, 4xH$_{2''}$), 7.83–7.82 (d, *J* = 8.5 Hz, 4H, 4xH$_{3''}$), 7.80 (s, 2H, 2xH$_{4'}$), 7.78 (s, 2H, 2xH$_{5'}$),

7.57–7.55 (d, J = 8.0 Hz, 2H, 2xH$_3$), 6.16 (s, 4H, 2xCH$_2$-β), 5.72 (s, 4H, 2xCH$_2$-α). ^{13}C-NMR (125 MHz, DMSO-*d6*) δ = 190.8 2xCO, 153.6 2xC$_2$, 138.9 C$_4$, 137.8 2xC$_{2'}$, 132.6 2xC$_{1''}$, 132.1 4xC$_{3''}$, 130.1 4xC$_{2''}$, 128.7 2xC$_{4''}$, 123.9 2xC$_{5'}$, 122.9 2xC$_{4'}$, 122.2 2xC$_3$, 55.6 2xCH$_2$-β, 52.6 2xCH$_2$-α. Anal. Calcd. for C$_{29}$H$_{25}$Br$_4$N$_5$O$_2$: C, 43.8; H, 3.17; N, 8.81; found: C, 43.7; H, 3.26; N, 9.01.

1,1′-(pyridine-2,6-diylbis(methylene))bis(3-(2-(4-chlorophenyl)-2-oxoethyl)-1H-imidazol-3-ium) bromide (4e)

Appearance: yellowish powder. Yield, 77%. mp 209–212°C. FTIR (KBr) cm^{-1} = 3126, 3086, 2972, 1697, 1589, 1558, 758. ^{1}H-NMR (500 MHz, DMSO-*d6*) δ = 9.23 (s, 2H, 2xH$_{2'}$), 8.05–8.02 (m, 5H, 4xH$_{2''}$, H$_4$), 7.78 (s, 2H, 2xH$_{4'}$), 7.76 (s, 2H, 2xH$_{5'}$), 7.69–7.67 (d, J = 8.5 Hz, 4H, 4xH$_{3''}$), 7.56–7.55 (d, J = 8.0 Hz, 2H, 2xH$_3$), 6.13 (s, 4H, 2xCH$_2$-β), 5.71 (s, 4H, 2xCH$_2$-α). ^{13}C-NMR (125 MHz, DMSO-*d6*) δ = 190.6 2xCO, 153.6 2xC$_2$, 139.4 2xC$_{4''}$, 138.9 C$_4$, 137.9 2xC$_{2'}$, 132.3 2xC$_{1''}$, 130.0 4xC$_{2''}$, 129.2 4xC$_{3''}$, 123.9 2xC$_{5'}$, 122.9 2xC$_{4'}$, 122.2 2xC$_3$, 55.6 2xCH$_2$-β, 52.7 2xCH$_2$-α. Anal. Calcd. for C$_{29}$H$_{25}$Br$_2$Cl$_2$N$_5$O$_2$: C, 49.32; H, 3.57; N, 9.92; found: C, 49.20; H, 3.67; N, 9.74.

1,1′-(pyridine-2,6-diylbis(methylene))bis(3-(2-(4-nitrophenyl)-2-oxoethyl)-1H-imidazol-3-ium) bromide (4f)

Appearance: pink powder. Yield, 81%. mp 233–236°C. FTIR (KBr) cm^{-1} = 3120, 2935, 1698, 1580, 1523, 1473, 1348. ^{1}H-NMR (500 MHz, DMSO-*d6*) δ = 9.31 (s, 2H, 2xH$_{2'}$), 8.40–8.39 (d, J = 9.0 Hz, 4H, 4xH$_{3''}$), 8.29–8.28 (d, J = 9.0 Hz, 4H, 4xH$_{2''}$), 8.05–8.02 (t, J = 8.0 Hz, 1H, H$_4$), 7.83–7.82 (add, 4H, 2xH$_{4'}$, 2xH$_{5'}$), 7.58–7.57 (d, J = 8.0 Hz, 2H, 2xH$_3$), 6.28 (s, 4H, 2xCH$_2$-β), 5.75 (s, 4H, 2xCH$_2$-α). ^{13}C-NMR (125 MHz, DMSO-*d6*) δ = 190.9 2xCO, 153.6 2xC$_2$, 150.4 2xC$_{4''}$, 138.9 C$_4$, 138.2 2xC$_{1''}$, 137.8 2xC$_{2'}$, 129.7 4xC$_{2''}$, 124.0 4xC$_{3''}$, 123.8 2xC$_{4'}$, 123.0 2xC$_{5'}$, 122.2 2xC$_3$, 56.0 2xCH$_2$-β, 52.7 2xCH$_2$-α. Anal. Calcd. for C$_{29}$H$_{25}$Br$_2$N$_7$O$_6$: C, 47.89; H, 3.46; N, 13.48; found: C, 47.99; H, 3.37; N, 13.65.

1,1′-(pyridine-2,6-diylbis(methylene))bis(3-(2-(4-methoxyphenyl)-2-oxoethyl)-1H-imidazol-3-ium) bromide (4g)

Appearance: white powder. Yield, 92%. mp 210–213°C. FTIR (KBr) cm^{-1} = 3076, 2933, 1683, 1600, 1244, 1168. ^{1}H-NMR (500 MHz, DMSO-*d6*) δ = 9.26 (s, 2H, 2xH$_{2'}$), 8.07–7.98 (m, 5H, H$_4$, 4xH$_{2''}$), 7.79–7.78 (ad, 4H, 2xH$_{4'}$, 2xH$_{5'}$), 7.57–7.56 (d, J = 7.5 Hz, 2H, 2xH$_3$), 7.11–7.09 (d, J = 8.5 Hz, 4H, 4xH$_{3''}$), 6.10 (s, 4H, 2xCH$_2$-β), 5.72 (s, 4H, 2xCH$_2$-α), 3.87 (s, 6H, 2xCH$_3$). ^{13}C-NMR (125 MHz, DMSO-*d6*) δ = 189.7 2xCO, 164.1 2xC$_{4''}$, 153.6 2xC$_2$, 138.9 C$_4$, 137.9 2xC$_{2'}$, 130.6 4xC$_{2''}$, 126.4 2xC$_{1''}$, 123.9 2xC$_{4'}$, 122.8 2xC$_{5'}$, 122.2 2xC$_3$, 114.3 4xC$_{3''}$, 55.7 2xCH$_3$, 55.2 2xCH$_2$-β, 52.6 2xCH$_2$-α. Anal. Calcd. for C$_{31}$H$_{31}$Br$_2$N$_5$O$_4$: C, 53.39; H, 4.48; N, 10.04; found: C, 53.26; H, 4.58; N, 9.86.

1,1′-(pyridine-2,6-diylbis(methylene))bis(3-(2-methoxy-2-oxoethyl)-1H-benzo[d]imidazol-3-ium) bromide (6a)

Appearance: white powder. Yield, 39%. mp 184–188°C. FTIR (KBr) cm^{-1} = 3135, 3080, 2933, 1729, 1600, 1431, 1234, 1069. ^{1}H-NMR (500 MHz, DMSO-*d6*) δ = 9.93 (s, 2H, 2xH$_{2'}$), 8.05–8.03 (m, 3H, 2xH$_{4'}$, H$_4$), 7.70–7.68 (d, J = 8.0 Hz, 2H, 2xH$_3$), 7.65–7.61 (t, J = 8.0 Hz, 4H, 2xH$_{7'}$, 2xH$_{5'}$), 7.44–7.41 (t, J = 8.0 Hz, 2H, 2xH$_{6'}$), 5.96 (s, 4H, 2xCH$_2$-α), 5.68 (s, 4H, 2xCH$_2$-β), 3.77 (s, 6H, 2xCH$_3$). ^{13}C-NMR (125 MHz, DMSO-*d6*) δ = 167.1 2xCO, 152.9 2xC$_2$, 143.7 2xC$_{2'}$, 139.0 C$_4$, 131.1 2xC$_{3'a}$, 130.5 2xC$_{7'a}$, 126.8 2xC$_{5'}$, 126.6 2xC$_{6'}$, 122.7 2xC$_3$, 113.9 2xC$_{4'}$, 113.5 2xC$_{7'}$, 52.9 2xCH$_3$, 50.7 2xCH$_2$-α, 47.5 2xCH$_2$-β. Anal. Calcd. for C$_{27}$H$_{27}$Br$_2$N$_5$O$_4$: C, 50.25; H, 4.22; N, 10.85; found: C, 50.10; H, 4.13; N, 11.04.

1,1′-(pyridine-2,6-diylbis(methylene))bis(3-(2-amino-2-oxoethyl)-1H-benzo[d]imidazol-3-ium) iodide (6b)

Appearance: yellow powder. Yield, 74%. mp 123–126°C. FTIR (KBr) cm^{-1} = 3349, 3168, 3040, 2915, 1680, 1598, 1420. ^{1}H-NMR (500 MHz, DMSO-*d6*) δ = 9.70 (s, 2H, 2xH$_{2'}$), 8.05–8.02 (m, 3H, H$_4$, 2x(-NH-)), 7.90–7.88 (d, J = 8.5 Hz, 2H, 2xH$_{4'}$), 7.72 (brs, 2H, 2x(-NH-)), 7.69–7.68 (d, J = 7.5 Hz, 2H, 2xH$_3$), 7.64–7.61 (t, J = 8.0 Hz, 2H, 2xH$_{5'}$), 7.60–7.59 (d, J = 8.0 Hz, 2H, 2xH$_{7'}$), 7.42–7.38 (t, J = 8.0 Hz, 2H, 2xH$_{6'}$), 5.89 (s, 4H, 2xCH$_2$-α), 5.26 (s, 4H, 2xCH$_2$-β). ^{13}C-NMR (125 MHz, DMSO-*d6*) δ = 166.4 2xCO, 152.9 2xC$_2$, 143.8 2xC$_{2'}$, 138.9 C$_4$, 131.2 2xC$_{3'a}$, 130.5 2xC$_{7'a}$, 126.6 2xC$_{5'}$, 126.4 2xC$_{6'}$, 122.6 2xC$_3$, 113.4 2xC$_{4'}$, 113.4 2xC$_{7'}$, 50.5 2xCH$_2$-α, 48.4 2xCH$_2$-β. Anal. Calcd. for C$_{25}$H$_{25}$I$_2$N$_7$O$_2$: C, 42.33; H, 3.55; N, 13.82; found: C, 42.43; H, 3.50; N, 13.97.

1,1′-(pyridine-2,6-diylbis(methylene))bis(3-(2-oxo-2-phenylethyl)-1H-benzo[d]imidazol-3-ium) bromide (6c)

Appearance: white powder. Yield, 50%. mp 203–205°C. FTIR (KBr) cm^{-1} = 3139, 2973, 1697, 1586, 1543, 1480. ^{1}H-NMR (500 MHz, DMSO-*d6*) δ = 9.88 (s, 2H, 2x$H_{2'}$), 8.12–8.11 (d, *J* = 8.0 Hz, 4H, 4x$H_{2''}$), 8.09–8.06 (m, 3H, H_4, 2x$H_{4'}$), 7.81–7.78 (t, *J* = 7.5 Hz, 2H, 2x$H_{4''}$), 7.75–7.73 (d, *J* = 8.0 Hz, 2H, 2xH_3), 7.68–7.59 (m, 8H, 2x$H_{7'}$, 4x$H_{3''}$, 2x$H_{5'}$), 7.45–7.42 (t, *J* = 8.0 Hz, 2H, 2x$H_{6'}$), 6.49 (s, 4H, 2xCH$_2$-β), 6.02 (s, 4H, 2xCH$_2$-α). ^{13}C-NMR (125 MHz, DMSO-*d6*) δ = 191.3 2xCO, 153.0 2xC_2, 143.8 2x$C_{2'}$, 139.0 C_4, 134.6 2x$C_{4''}$, 133.6 2x$C_{1''}$, 131.6 2x$C_{3'a}$, 130.5 2x$C_{7'a}$, 129.0 4x$C_{3''}$, 128.5 4x$C_{2''}$, 126.7 2x$C_{5'}$, 126.5 2x$C_{6'}$, 122.7 2xC_3, 113.9 2x$C_{4'}$, 113.4 2x$C_{7'}$, 53.4 2xCH$_2$-β, 50.7 2xCH$_2$-α. Anal. Calcd. for $C_{37}H_{31}Br_2N_5O_2$: C, 60.26; H, 4.24; N, 9.50; found: C, 60.16; H, 4.33; N, 9.35.

1,1′-(pyridine-2,6-diylbis(methylene))bis(3-(2-(4-bromophenyl)-2-oxoethyl)-1H-benzo[d]imidazol-3-ium) bromide (6d)

Appearance: white powder. Yield, 77%. mp 193–195°C. FTIR (KBr) cm^{-1} = 3140, 3020, 2943, 1694, 1585, 1550, 1470, 620. ^{1}H-NMR (500 MHz, DMSO-*d6*) δ = 9.83 (s, 2H, 2x$H_{2'}$), 8.08–8.05 (m, 3H, H_4, 2x$H_{4'}$), 8.02–8.01 (d, *J* = 9.0 Hz, 4H, 4x$H_{2''}$), 7.87–7.85 (d, *J* = 8.5 Hz, 4H, 4x$H_{3''}$), 7.74–7.72 (d, *J* = 7.5 Hz, 2H, 2xH_3), 7.68–7.66 (d, *J* = 8.5 Hz, 2H, 2x$H_{7'}$), 7.62–7.59 (t, *J* = 7.5 Hz, 2H, 2x$H_{5'}$), 7.46–7.43 (t, *J* = 7.5 Hz, *J* = 8.0 Hz, 2H, 2x$H_{6'}$), 6.43 (s, 4H, 2xCH$_2$-β), 6.00 (s, 4H, 2xCH$_2$-α). ^{13}C-NMR (125 MHz, DMSO-*d6*) δ = 190.7 2xCO, 153.0 2xC_2, 143.8 2x$C_{2'}$, 139.0 C_4, 132.6 2x$C_{1''}$, 132.1 4x$C_{3''}$, 131.6 2x$C_{3'a}$, 130.5 2x$C_{7'a}$, 130.4 4x$C_{2''}$, 128.8 2x$C_{4''}$, 126.7 2x$C_{5'}$, 126.5 2x$C_{6'}$, 122.7 2xC_3, 114.0 2x$C_{4'}$, 113.4 2x$C_{7'}$, 53.3 2xCH$_2$-β, 50.7 2xCH$_2$-α. Anal. Calcd. for $C_{37}H_{29}Br_4N_5O_2$: C, 49.64; H, 3.26; N, 7.82; found: C, 49.74; H, 3.17; N, 7.98.

1,1′-(pyridine-2,6-diylbis(methylene))bis(3-(2-(4-chlorophenyl)-2-oxoethyl)-1H-benzo[d]imidazol-3-ium) bromide (6e)

Appearance: white powder. Yield, 83%. mp 175–178°C. FTIR (KBr) cm^{-1} = 3136, 3068, 2970, 1695, 1589, 1564, 1483, 765. ^{1}H-NMR (400 MHz, DMSO-*d6*) δ = 9.84 (2H, s, 2x$H_{2'}$), 8.11–8.09 (d, *J* = 8.4 Hz, 4H, 4x$H_{2''}$), 8.07–8.05 (d, *J* = 8.0 Hz, 3H, 2x$H_{4'}$, H_4), 7.74–7.67 (m, 8H, 2xH_3, 4x$H_{3''}$, 2x$H_{7'}$), 7.63–7.59 (t, *J* = 7.6 Hz, 2H, 2x$H_{5'}$), 7.46–7.42 (t, *J* = 7.6 Hz, 2H, 2x$H_{6'}$), 6.44 (s, 4H, 2xCH$_2$-β), 6.00 (s, 4H, 2xCH$_2$-α). ^{13}C-NMR (100 MHz, DMSO-*d6*) δ = 190.4 2xCO, 153.0 2xC_2, 143.8 2x$C_{2'}$, 139.5 2x$C_{4''}$, 139.0 C_4, 132.3 2x$C_{1''}$, 131.6 2x$C_{3'a}$, 130.5 2x$C_{7'a}$, 130.3 4x$C_{2''}$, 129.1 4x$C_{3''}$, 126.7 2x$C_{5'}$, 126.5 2x$C_{6'}$, 122.7 2xC_3, 113.9 2x$C_{4'}$, 113.4 2x$C_{7'}$, 53.4 2xCH$_2$-β, 50.7 2xCH$_2$-α. Anal. Calcd. for $C_{37}H_{29}Br_2Cl_2N_5O_2$: C, 55.11; H, 3.62; N, 8.69; found: C, 54.96; H, 3.57; N, 8.85.

1,1′-(pyridine-2,6-diylbis(methylene))bis(3-(2-(4-nitrophenyl)-2-oxoethyl)-1H-benzo[d]imidazol-3-ium) bromide (6f)

Appearance: yellowish powder. Yield, 48%. mp 235–238°C. FTIR (KBr) cm^{-1} = 3135, 3018, 2955, 1685, 1583, 1525, 1488, 1348. ^{1}H-NMR (500 MHz, DMSO-*d6*) δ = 9.88 (s, 2H, 2x$H_{2'}$), 8.43–8.42 (d, *J* = 8.0 Hz, 4H, 4x$H_{3''}$), 8.35–8.33 (d, *J* = 8.5 Hz, 4H, 4x$H_{2''}$), 8.12–8.06 (m, 3H, 2x$H_{4'}$, H_4), 7.75–7.73 (d, *J* = 7.5 Hz, 2H, 2xH_3), 7.71–7.70 (d, *J* = 8.5 Hz, 2H, 2x$H_{7'}$), 7.64–7.61 (t, *J* = 7.5 Hz, 2H, 2x$H_{5'}$), 7.48–7.45 (t, *J* = 7.5 Hz, 2H, 2x$H_{6'}$), 6.55 (s, 4H, 2xCH$_2$-β), 6.03 (s, 4H, 2xCH$_2$-α). ^{13}C-NMR (125 MHz, DMSO-*d6*) δ = 190.7 2xCO, 153.0 2xC_2, 150.5 2x$C_{4''}$, 143.7 2x$C_{2'}$, 139.0 C_4, 138.3 2x$C_{1''}$, 131.6 2x$C_{3'a}$, 130.5 2x$C_{7'a}$, 130.0 4x$C_{2''}$, 126.7 2x$C_{5'}$, 126.6 2x$C_{6'}$, 123.9 4x$C_{3''}$, 122.7 2xC_3, 114.1 2x$C_{4'}$, 113.5 2x$C_{7'}$, 53.9 2xCH$_2$-β, 50.7 2xCH$_2$-α. Anal. Calcd. for $C_{37}H_{29}Br_2N_7O_6$: C, 53.70; H, 3.53; N, 11.85; found: C, 53.80; H, 3.62; N, 11.70.

1,1′-(pyridine-2,6-diylbis(methylene))bis(3-(2-(4-methoxyphenyl)-2-oxoethyl)-1H-benzo[d]imidazol-3-ium) bromide (6g)

Appearance: white powder. Yield, 71%. mp 183–186°C. FTIR (KBr) cm^{-1} = 3138, 3016, 2931, 1683, 1599, 1566, 1242, 1172. ^{1}H-NMR (500 MHz, DMSO-*d6*) δ = 9.89 (s, 2H, 2x$H_{2'}$), 8.08–8.04 (m, 7H, 4x$H_{2''}$, 2x$H_{4'}$, H_4), 7.76–7.75 (d, *J* = 7.5 Hz, 2H, 2xH_3), 7.70–7.68 (d, *J* = 8.0 Hz, 2H, 2x$H_{7'}$), 7.62–7.58 (t, *J* = 8.0 Hz, 2H, 2x$H_{5'}$), 7.45–7.42 (t, *J* = 8.0 Hz, 2H, 2x$H_{6'}$), 7.14–7.12 (d, *J* = 8.5 Hz, 4H, 4x$H_{3''}$), 6.42 (s, 4H, 2xCH$_2$-β), 6.01 (s, 4H, 2xCH$_2$-α), 3.90 (6H, s, 2xCH$_3$). ^{13}C-NMR (125 MHz, DMSO-*d6*) δ = 189.5 2xCO, 164.2 2x$C_{4''}$, 153.0 2xC_2, 143.8 2x$C_{2'}$, 139.0 C_4, 131.6 2x$C_{3'a}$, 130.9 4x$C_{2''}$, 130.5 2x$C_{7'a}$, 126.6 2x$C_{5'}$, 126.5 2x$C_{6'}$, 126.4 $C_{1''}$, 122.7 2xC_3, 114.2 4x$C_{3''}$, 113.9 2x$C_{4'}$, 113.4 2x$C_{7'}$, 55.8 2xCH$_3$, 53.0 2xCH$_2$-β, 50.6 2xCH$_2$-α. Anal. Calcd. for $C_{39}H_{35}Br_2N_5O_4$: C, 58.73; H, 4.42; N, 8.78; found: C, 58.63; H, 4.47; N, 8.63.
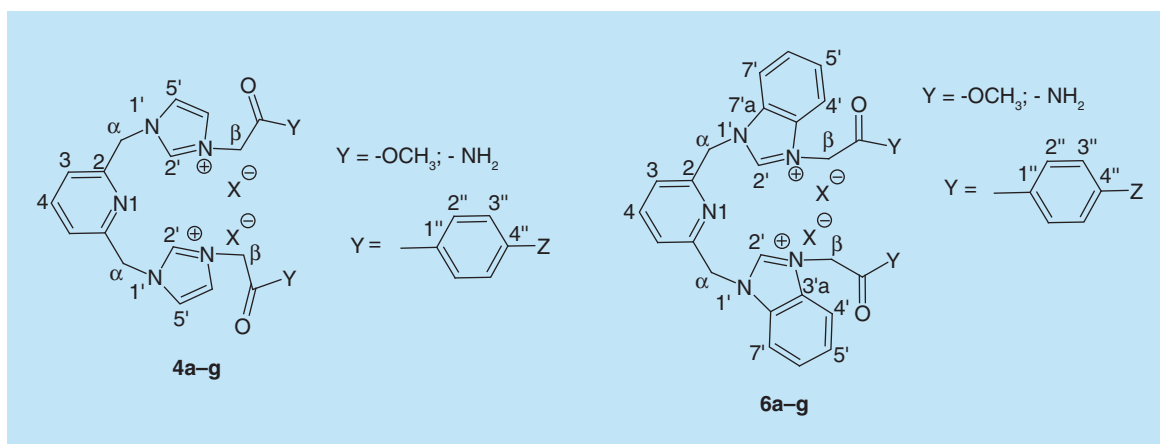
Figure 1.   Atom identification in the spectral data of quaternary salts 4a–g and 6a–g.

Microbiology

Compounds were evaluated for antimycobacterial activity against *Mycobacterium tuberculosis*, as a part of the Center of Tuberculosis Antimicrobial Acquisition and Coordinating Facility (TAACF) TB screening program under direction of the US National Institute of Health, the NIAID division. Antimycobacterial activities of the compounds were performed by TAACF at Southern Research Institute. All protocols concerning the antimycobacterial evaluation of tested compounds can be found in the Supplementary Figure 1.

Results & discussion

Design & synthesis

One of the most useful strategies in drug discovery is the pharmacophore combination of well defined scaffolds. Bearing in mind this strategy, we decided to bring new contributions in the anti-TB fighting and, pursuing to achieve products with better activity, better pharmacological properties and alternative mechanisms of action, the present study is aimed to combine three pharmacophores: pyridine, imidazole/benzimidazole and *p*-chlorobenzoyl moieties. Structural necessities around pyridine and imidazole/benzimidazole moieties, for an anti-TB activity, are depicted in Figure 2.

The first two pharmacophores units, pyridine and imidazole/benzimidazole moieties, are connected via a methylene (-CH$_2$-) linker in 2,6- position of pyridine, respectively 1-position of imidazole/benzimidazole, the BIP derivatives type I being obtained. The *p*-chlorobenzoyl moiety was found to be a potent pharmacophoric unit for the antimycobacterial activity and also a useful antibacterial pharmacophore (due to its high lipophilicity) [19,24,25]. Consequently, we decide to anchor the *p*-chlorobenzoyl moiety in the 3-position of imidazole/benzimidazole, a second class of BIP derivatives, type II being obtained. We also decided to study the influence of other *p*-substituted (-H, -NO$_2$, -OMe)-benzoyl moieties and nonbenzoyl moiety (-carbalkoxy, -acetamide) anchored to imidazole/benzimidazole, in order to allow structure–activity relationship (SAR) comparisons with *p*-chlorobenzoyl moiety.

In order to synthesize the BIP derivatives a direct approach was used, involving only two successive *N*-alkylations (Figure 3). A first *N*-alkylation of NH- imidazolic unit (from imidazole, 4-nitroimidazole and benzimidazole) is leading to the corresponding BIP derivatives type I, **2a, b** and **5**. The second alkylation consists in a quaternization reaction of *N3*-nitrogen atom from the imidazolic moiety with variously activated halogenated derivatives type **3** (2–bromo/iodo-alkyl esters/amide **3a, b** or ϖ–bromo *p*-Z-substituted-acetophenones **3c–g**), the BIP derivatives type II, **4a–g** and **6a–g**, being obtained.

For the BIP compound **2b**, the quaternization reaction of *N3*-nitrogen atom from imidazole does not occur, the most probable because the imidazole ring is too deactivated (Figure 4).

Using the modern tools of structural organic analysis (IR, ^{1}H-NMR, ^{13}C-NMR, 2D-COSY, 2D-HMQC, 2D-HMBC, and elemental analysis: C, H, N), we proved equivocally the structure of our compounds. In our structural organic analysis, we considered compound **6e** as representative for the BIP derivatives (is the most active and promising anti-TB compound). The most informative signals furnished by ^{1}H-NMR spectrum of **6e** are
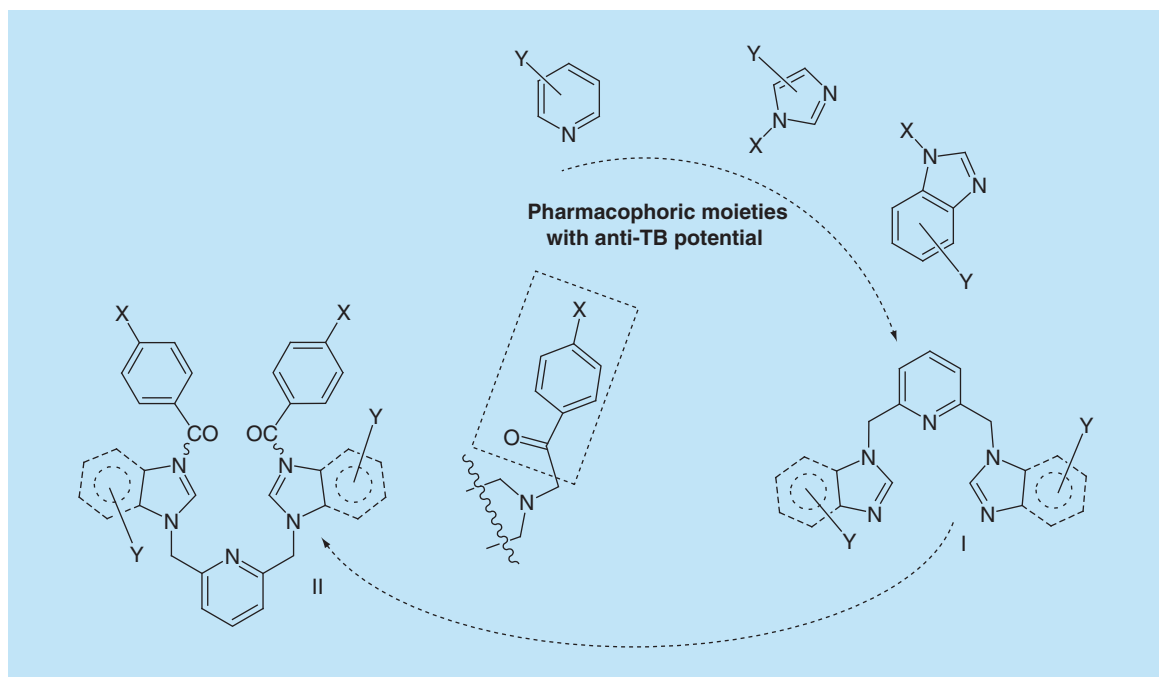
Figure 2.   Design in the class of *bis*-(imidazole/benzimidazole)-pyridine derivatives.
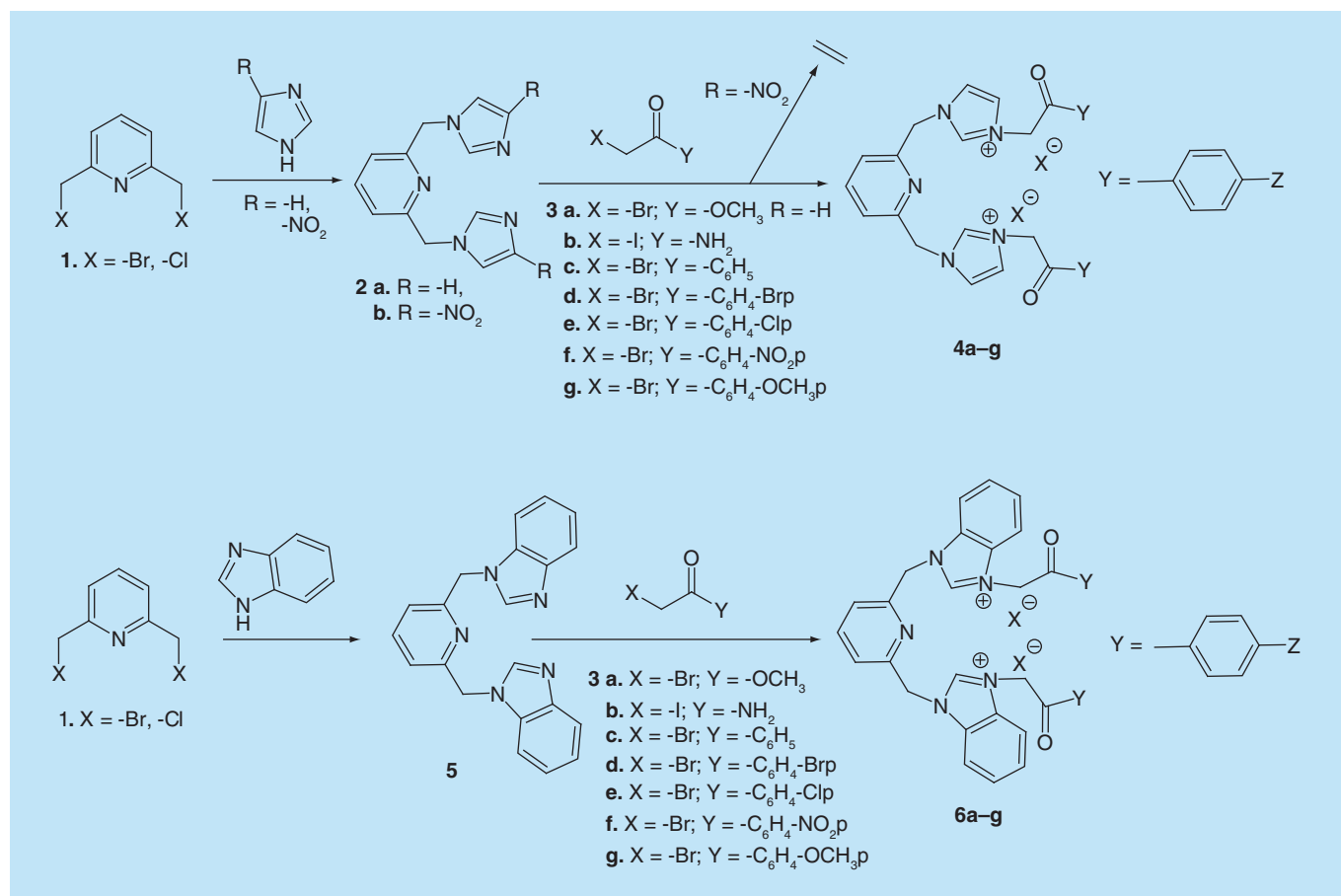

Figure 3.   Reaction pathway to obtain *bis*-imidazole/benzimidazole-pyridine derivatives.
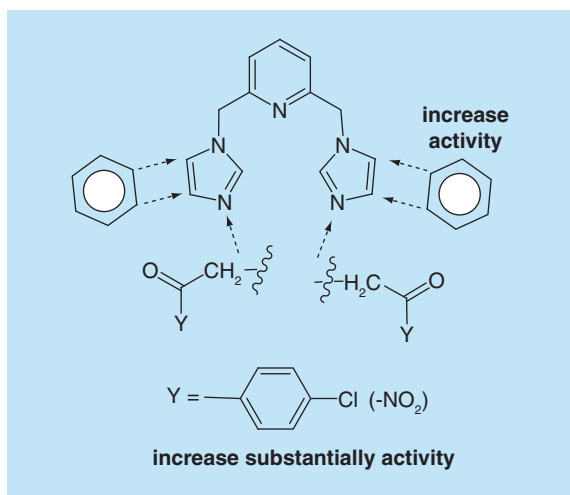
Figure 4.   Structure–activity relationship correlations in the class of *bis*-(imidazole/benzimidazole)-pyridine derivatives.

those one of the aromatic protons H2′ (from imidazole ring) and H2″ (from benzoyl), respectively the methylene protons: 2H (CH_2-α pyridine) and 2H (CH_2-β benzoyl). The most deshielded protons are H2′ (9.84 p.p.m., singlet) from benzimidazole moiety, due to the powerful deshielding effect of the positive nitrogen atom *N3′* and *N1′* nitrogen. The next deshielded protons are H2″ from benzoyl moiety (8.11–8.09 p.p.m., doublet, *J* = 8.4 Hz), being deshielded by the electron withdrawing effect of the adjacent carbonyl ketone group and *p*-chlorophenyl moiety. The signals of the two methylene groups appear as singlet, at a very low field, unusual for this type of protons: 6.44 p.p.m. (CH_2-β benzoyl) and 6.00 p.p.m. (CH_2-α pyridine). This situation could be explained by the powerful electron withdrawing effect exerted by the CO carbonyl group and positive nitrogen atom *N3′* from imidazole moiety (for CH_2-β) from proximity, respectively nitrogen atom *N1′* from imidazole and α-pyridine ring (for CH_2-α).

In the ^{13}C-NMR spectrum, the most important data are furnished by the signals corresponding to the carbonyl group, C2 (from pyridine), C2′ (from imidazole ring) and the two carbons from the methylene groups (CH_2-α pyridine and CH_2-β benzoyl). The signals for carbonyl group appear at 190.4 p.p.m., typical for a C = O carbonyl ketone group. The C2 carbon is strongly deshielded (appears at 153.0 p.p.m.), being a α-endocyclic carbon from pyridine moiety. The C2′ carbon is also strongly deshielded (appears at 143.8 p.p.m.), in accordance with the powerful deshielding effect of the two adjacent nitrogen atoms from imidazole ring. The carbons from methylene groups appear at unusual low field: 53.4 p.p.m. (carbon from CH_2-β benzoyl) and 50.7 p.p.m. (carbon from CH_2-α pyridine). The same explications as far for methylene protons remain valid. The other remaining peaks form NMR spectra fully confirm the structure of compounds. Additional information concerning the ^{1}H- and ^{13}C-NMR spectra of compound **6e** is shown in the Supplementary Information.

Antimycobacterial assay against *Mycobacterium tuberculosis*

The obtained compounds have been evaluated for their *in vitro* antimycobacterial activity against *Mtb* H37Rv (grown under aerobic conditions), on TAACF, US NIH, the NIAID division, at Southern Research Institute. The first step of assay consisted in the determination of relative solubility of our products in microbiological medium using turbidity as a standard parameter [32]. The results listed in Table 1 show that all the BIP compounds are soluble at the highest concentration (200 μM). For a future drug candidate, this excellent solubility microbiological medium is an excellent strength.

Further, the *in vitro* screening assay allowed to determine the minimum inhibitory concentration (MIC), IC_{50} and IC_{90} (the concentrations that resulted in 50% and 90% inhibition of growth; Table 1) [33–37].

As can be seen, eight (**2b**, **5**, **4e**, **4f**, **6c**, **6e**, **6f** and **6g**) from the 15 tested compounds had activity against *Mtb* H37Rv under aerobic conditions, with a MIC in the range of 17– 92 μM, and an IC_{50} in the range of 7.9 – 77 μM. From SAR point of view, the following remarks could be done: the BIP II compounds are more active than BIP I, which means that anchoring of a *p*-substituted-benzoyl moiety in the 3-position of imidazole/benzimidazole moiety is favorable for activity; the compounds bearing a benzimidazole moiety are more active than those one bearing an imidazole moiety. Compound **6e** (with a *p*-chlorobenzoyl moiety anchored to benzimidazole) have

Table 1. Solubility in microbiological medium and antimycobacterial activity of *bis*-(imidazole/benzimidazole)-pyridine compounds against *Mtb* H37Rv under aerobic conditions.					
Compound	MIC (μM)	IC$_{50}$ (μM)	IC$_{90}$ (μM)	Compound solubility	
				Starting concentration (μM)	Lowest insoluble concentration (μM)
2a	>200	>200	>200	200	N/A
2b[†]	92	77	100	200	N/A
4a	>200	>200	>200	200	N/A
4b	>200	>200	>200	200	N/A
4c	>200	>200	>200	200	N/A
4e[†]	51	34	63	200	N/A
4f[†]	58	38	71	200	N/A
4g	>200	160	>200	200	N/A
5[†]	>50	43	>50	200	N/A
6a	>200	>200	>200	200	N/A
6b	>200	180	>200	200	N/A
6c[†]	56	25	60	200	N/A
6e[†]	17	7.9	18	200	N/A
6f[†]	24	14	21	200	N/A
6g[†]	58	28	6	200	N/A
Rifam picin	0.0060	0.0036	0.070	0.04	N/A

[†]Values indicate that compounds have a very good activity.
IC$_{50}$: 50% inhibition of growth; IC$_{90}$: 90% inhibition of growth; N/A: Compound was soluble at the highest concentration; MIC: Minimum inhibitory concentration.

Table 2. Activity against *Mtb* H37Rv at lower starting concentrations for *bis*-(imidazole/benzimidazole)-pyridine derivatives 2b, 5, 4f, 6c and 6f.			
Compound	MIC aerobic condition (μM)	IC$_{50}$ (μM)	IC$_{90}$ (μM)
2b [†]	101	93	100
5	>50	>50	>50
4f[†]	104	45	140
6c[†]	87	34	110
6f[†]	16	11	20
Rifampicin	0.0063	0.0040	0.0077

[†]Values indicate that compounds have a very good activity.
IC$_{50}$: 50% inhibition of growth; IC$_{90}$: 90% inhibition of growth; MIC: Minimum inhibitory concentration.

shown the most pronounced antimycobacterial activity, which confirms our initial design considerations; and the *p*-substituted-benzoyl compounds are more much active than nonbenzoyl substituted (-carbalkoxy, -acetamide). Also, the active compounds are those one having in the para position of benzoyl moiety a chloride or nitro group, while replacing them with other atoms or group of atoms is leading to a dropping of antimycobacterial activity.

Five BIPderivatives, namely **2b, 5, 4f, 6c** and **6f**, with showed the best anti-TB profile in the primary assay, was passed into the secondary assays for evaluation of antimcyobacterial activity in a low throughput format. These assays include a revaluation of MIC, IC$_{50}$ and IC$_{90}$ against *Mtb* H37Rv grown under aerobic conditions, MIC under low oxygen, minimal bactericidal concentration (MBC), testing on drug-resistant *Mtb*, intracellular activity and cytotoxicity.

Initially, MIC, IC$_{50}$ and IC$_{90}$ were repeated at lower starting concentrations (Table 2). As we may notice from Table 2, the results of assay are reproducible, the obtained values being comparable with the previous ones listed in Table 1.

The bactericidal activity of BIP derivatives was determined subsequent to MIC assay. The MBC assay determines whether a drug's mechanism of action is bacteriostatic or bactericidal. A bactericidal mechanism of action is a truly advantage of drug candidates, because could shorten the standard treatment of TB with a minimum of 6 months. The MBC was determined against *Mtb H37Rv* grown in aerobic conditions, and indicate that three of the tested

Table 3. Minimal bactericidal concentration assay for compounds 2b, 5, 4f, 6c and 6f.

Compound	MIC (μM)	MBC (μM)	Concentration dependent	Time dependent
2b[†]	92	>200	ND	ND
4f[†]	58	100	N	Y
5	>50	>50	ND	ND
6c[†]	56	100	Y	N
6f[†]	18	50	Y	N

[†]Values indicate that compounds have a very good activity.
MBC: Minimal bactericidal concentration; MIC: Minimum inhibitory concentration; N: No; ND: Not determined; Y: Yes.

Table 4. Low oxygen recovery assay for compounds 2b, 5, 4f, 6c and 6f.

Compound	Low oxygen			Normal oxygen		
	MIC (μM)	IC_{50} (μM)	IC_{90} (μM)	MIC (μM)	IC_{50} (μM)	IC_{90} (μM)
2b[†]	200	26	91	>200	>200	>200
5	>50	>50	>50	>50	>50	>50
4f[†]	183	25	65	129	49	78
6c[†]	200	16	130	>200	17	60
6f[†]	120	9.7	33	71	9.9	25
Rifampicin	0.13	0.0041	0.0065	0.096	0.0072	0.0025
Metronidazole	200	29	110	>200	>200	>200

[†]Values indicate that compounds have a very good activity.
IC_{50}: 50% inhibition of growth; IC_{90}: 90% inhibition of growth; MIC: Minimum inhibitory concentration.

compounds (**4f**, **6c**, **6f**) have a bactericidal mechanism of action, Table 3. We may also notice from Table 3 that the activity of compounds **6c** and **6f**, are concentration dependent, which is associated with an optimal free drug maximum concentration to MIC ratio [38]. In the case of **4f** molecule, a time dependent effect is observed, which is usually linked with a free drug concentrations existing above the MIC for a certain section of the dosing interval [38].

Low oxygen recovery assay are furnishing essential information concerning activity against *Mtb* in a state of nonreplicating persistence (NRP). Nonreplicating state of *Mtb* is responsible for antimicrobial tolerance found in more and more cases of TB infections. As a result, the antimycobacterial activity against NRP *Mtb* H37Rv for compounds **2b, 5, 4f, 6c** and **6f**, were determined [39–41]. Results for the low oxygen recovery assay in terms of MIC, IC_{50} and IC_{90}, are listed in Table 4.

As can be seen in Table 4, our compounds (except **5**) had activity against NRP *Mtb* H37Rv superior to control metronidazole, with an IC_{50} in the range of 9.7– 26 μM, and a MIC in the range of 120–200 μM.

Next, MIC, IC_{50} and IC_{90} of compounds **2b, 5, 4f, 6c** and **6f** against five resistant isolates of *Mtb* strains [34–37] and nontuberculous mycobacteria (NTM) [34,37,42] under aerobic conditions were determined, Table 5.The NTM were *Mycobacterium avium* and *Mycobacterium abscessus*, while the resistant isolates were INH-R1 and INH-R2 (strains resistant to isoniazid), RIF-R1 and RIF-R2 (strains resistant to rifampicin), and FQ-R1 (strain resistant to fluoroquinolone).

The data from Table 5 indicate that *Mtb* monoresistant isolates were not resistant to our compounds (except **5**) and, compounds **4f, 6c** and **6f** showed activity against *M. abscessus*, while against *M. avium* only compound **6f** showed a moderate activity.

The cytotoxicity of BIP compounds were established by using the THP-1 human monocytic cell line [40], and measuring the IC_{50} values. Similar, the activity of compounds against intracellular *Mtb* H37Rv were determined by measuring viability in infected THP-1 cell line [40], and expressed in terms of IC_{50} and IC_{90}, values. The obtained results are listed in Table 7.

As can be seen in Table 7, all our compounds are not cytotoxic and all tested compounds exhibited a very good intracellular activity, those one of compound **6f** being remarkable. The data presented before indicate that compound **6f** have a promising anti-TB profile and, as a result, a study concerning absorption, distribution, metabolism, excretion and toxicity (ADMET) have been done. The ADMET study begin with plasma–protein binding assay of compound **6f**, using equilibrium dialysis method with a semipermeable membrane, which separates two compartments containing protein (human plasma) and buffer [43,44]. The obtained results are listed in Table 8.

Table 5. MIC, IC_{50} and IC_{90} of compounds 2b, 5, 4f, 6c and 6f against *Mtb* resistant at different treatment and nontuberculous mycobacteria.

Compound	INH-R1			INH-R2			RIF-R1			*Mycobacterium avium*
	MIC (μM)	IC_{50} (μM)	IC_{90} (μM)	MIC (μM)	IC_{50} (μM)	IC_{90} (μM)	MIC (μM)	IC_{50} (μM)	IC_{90} (μM)	MIC (μM)
2b[†]	98	68	90	28	24	28	111	60	160	–
5	>50	>50	>50	>50	>50	>50	>50	>50	>50	–
4f[†]	55	46	52	65	39	75	67	35	100	>200
6c[†]	120	42	170	110	42	150	87	24	110	>200
6f[†]	24	13	21	25	13	22	25	15	24	200
C1	0.018	0.0084	0.022	0.065	0.0047	0.012	2	1.2	2.3	>200
C2	>200	>200	>200	>200	>200	>200	0.17	0.15	0.21	–
C3	1.2	0.64	1.4	1.4	0.84	1.4	0.76	0.59	0.91	–

[†]Values indicate that compounds have a very good activity.
C1: Rifampicin control; C2: Isoniazid control; C3: Levofloxacin control; FQ: Fluoroquinolone resistant strain; IC_{50}: 50% inhibition of growth; IC_{90}: 90% inhibition of growth; INH: Isoniazid resistant strain; MIC: Minimum inhibitory concentration; RIF: Rifampicin resistant strain.

Table 6. MIC, IC_{50} and IC_{90} of compounds 2b, 5, 4f, 6c and 6f against *Mtb* resistant at different treatment and nontuberculous mycobacteria.

Compound	RIF-R2			FQ-R1			*Mycobacterium abscessus*		
	MIC (μM)	IC_{50} (μM)	IC_{90} (μM)	MIC (μM)	IC_{50} (μM)	IC_{90} (μM)	MIC (μM)	IC_{50} (μM)	IC_{90} (μM)
2b	68	38	61	102	66	92	–	–	–
5	>50	>50	>50	>50	>50	>50	–	–	–
4f[†]	>200	40	120	87	49	91	110	89	97
6c[†]	100	44	120	200	40	>200	>200	120	200
6f[†]	30	17	31	38	18	38	88	56	68
C1	>50	>50	>50	0.027	0.013	0.039	3.3	2.1	3.1
C2	0.62	0.54	0.60	0.35	0.36	0.47	–	–	–
C3	1.1	0.60	1.2	20	12	22	–	–	–

[†]Values indicate that compounds have a very good activity.
C1: Rifampicin control; C2: Isoniazid control; C3: Levofloxacin control; FQ: Fluoroquinolone resistant strain; INH: Isoniazid resistant strain; MIC: Minimum inhibitory concentration; RIF: Rifampicin resistant strain.

Table 7. Intracellular activity and cytotoxicity evaluation.

Compound	Cytotoxicity IC_{50} (μM)	IC_{50} intracell (μM)	IC_{90} intracell (μM)
2b[†]	>50	>200	>200
5[†]	>50	>200	>200
4f[†]	>50	26	48
6c[†]	>50	37	>50
6f[†]	>50	14	26
Control compound[‡,§]	0.018[‡]	0.23[§]	0.29[§]

[†]Bold and italic values indicate that compounds have a very good activity.
[‡]Staurosporine control.
[§]Isoniazid control.
IC_{50}: 50% inhibition of growth; IC_{90}: 90% inhibition of growth.

Table 8. Results of plasma–protein binding for compound 6f.

Compound	Test species	Mean plasma fraction unbound (%)	Mean plasma fraction bound (%)	Recovery
6f	Human	7.8	92.2	24.5
Propranolol[†]	Human	20.7	79.3	93
Warfarin[†]	Human	0.51	99.5	96.7

[†]Control compounds: propranolol (normal binding) and warfarin (high-binding).

Table 9. Results of Caco-2 assay of compound 6f.

Compound	Mean A→B P_{app}[†] (10^{-6} cm/s)	Mean B→A P_{app}[†] (10^{-6} cm/s)	Efflux ratio[‡]
6f	0.47	0.095	0.20
Atenolol[§]	0.13	0.37	2.8
Propranolol[§]	12.7	25	2
Talinolol[§]	0.077	3.3	43

[†] Papp is the apparent permeability;
[‡] Efflux ratio (Re) is P_{app} (B→A)/P_{app} (A→B);
[§] Control compounds.

Table 10. Results of cytochrome P450 inhibition for compound 6f.

Compound	IC$_{50}$ (μM)						
	CYP3A4 – midazolam	CYP3A4 – testosterone	CYP2C9	CYP2D6	CYP2C8	CYP2B6	CYP2C19
6f	>20	6.6	>20	0.92	>20	>20	8.8
Ketoconazole[†]	0.033	0.022	–	–	–	–	–
Sulfaphenazole[†]	–	–	0.16	–	–	–	–
Quinidine[†]	–	–	–	0.032	–	–	–
Montelukast[†]	–	–	–	–	0.14	–	–
Tranylcypromine[†]	–	–	–	–	–	–	7.5
Ticlopidine[†]	–	–	–	–	–	0.72	–

[†] Control compounds.
IC$_{50}$: 50% inhibition of growth.

As it could be seen in Table 8, compound **6f** have a value of plasma fraction bound lesser than 95% (92.2%), which means a lower clearance rate and a greater half-time *in vivo* and, consequently a more efficacy because of higher free drug concentration. The absorption properties of compound **6f** through the intestinal epithelium were studied using the Caco-2 cell monolayer permeability assay, measuring in both directions (apical to basal, respectively basal to apical) the permeability of compound **6f** [45–49]. The obtained results are listed in Table 9.

The low active efflux (R*e* = 0.20) and low permeability (A→B P_{app} <2), indicate that compound **6f** is poorly permeable and suggest a mechanism of absorption almost paracellular, with basically no involvement of transporter proteins (P-glycoprotein or others).

The early discovery of the potential drug–drug interactions is a necessary clue to increase the safety of pharmacotherapy, the drug–drug interactions being associated with the increasing of toxicity, decrease of pharmacological effect and adverse drug reactions [50]. One of the best methods used for detection of drug–drug interactions consist in drug metabolism determination *via* the cytochrome P450 system. In this respect, compound **6f** was tested on while the resistant isolates were INH-R1 and INH-R2 (strains resistant to isoniazid), RIF-R1 and RIF-R2 (strains resistant to rifampicin), and FQ-R1 (strain resistant to fluoroquinolone; Table 10) [50–52].

Compound **6f** did not show inhibition (IC$_{50}$ >20) on CYP3A4 – midazolam, CYP2C9, CYP2C8, CYP2B6 and have a low to moderate inhibition (IC$_{50}$: 6.6 and 8.8) on CYP3A4 – testosterone and CYP2C19, these results indicating a low potential for drug–drug interactions. The microsomal binding assay is another important parameter in the prediction of *in vivo* pharmacokinetics from *in vitro* drug metabolism data. In order to determine microsomal stability of compounds, the assay is using pooled human liver S9 microsomes in the presence of the co-factor NADPH [53–55]. The obtained results are listed in Table 11.

The data from Table 11 indicate that compound **6f** is a low cleared compound, having a CL$_{int}$ <50 μl/min/mg. These indicate that compound **6f** is likely to be slowly cleared *in vivo*, resulting in a higher duration of action. Finally, the cytotoxicity of compound **6f** was determined on human liver cells (HepG2), using staurosporine as control (IC$_{50}$ = 0.0086 μM) [56–59]. Compound **6f** showed an IC$_{50}$ >100 μM, having no cytotoxicity.

Conclusion

In summary, we report herein the design, synthesis and antimycobacterial activity of two new classes of BIP derivatives. The reaction pathway is advantageous and straight applicable, with two steps only: a *N1*-alkylations

Table 11. *In vitro* microsomal stability assay of compound 6f.						
Compound	C (μM)	Test species	NADPH-dependent CL$_{int}$[†] (μl/min/mg)	NADPH-dependent T$_{1/2}$[‡] (min)	NADPH-free CL$_{int}$[†] (μl/min/mg)	NADPH-free T$_{1/2}$[‡] (min)
6f	1	Human	21.7	106	<12.8	>180
Verapamil	1	Human	123	18.7	<12.8	>180
Dextromethorphan	1	Human	24.3	94.9	<12.8	>180

[†] Microsomal intrinsic clearance = ln(2)/(T$_{1/2}$[microsomal protein]).
[‡] Half-life = 0.693/-k, where k is the rate constant.

followed by a quaternization reaction of *N3*-nitrogen atom from the imidazolic moiety. 15 of the newly synthesized compounds were subject to the primary antimycobacterial assay against *M. tuberculosis* H37Rv under aerobic conditions, and reveal that eight (**2b**, **5**, **4e**, **4f**, **6c**, **6e**, **6f** and **6g**) from the tested compounds had activity against *Mtb* H37Rv. SAR correlations indicate that the most valuable compounds are belong to the BIP **II** class, which prove that anchoring of a *p*-substituted-benzoyl moiety in the 3-position of imidazole/benzimidazole moiety is favorable for activity. From these, the most active compounds are those one having in the *para* position of benzoyl moiety a chloride or nitro group. All BIP compounds proved to be with excellent solubility in microbiological medium, which is an excellent strength for a future drug candidate. The best anti-TB five compounds (**2b**, **5**, **4f**, **6c** and **6f**) was subject to the secondary antimycobacterial screening, these assay indicating that our compounds are potent against both replicating and nonreplicating *Mtb* (superior to control metronidazole), posses a very good intracellular activity (those one of compound **6f** being the highest), are active against drug-resistant *Mtb* strains, and have no cytotoxicity (on eukaryotic THP-1 human monocytic cells). Three of the tested compounds (**4f**, **6c**, **6f**) have a bactericidal mechanism of action and present a moderate to good activity against NTM. The pharmacokinetic ADMET screening of **6f**, indicate a lower clearance rate, a great half-time *in vivo*, a low potential for drug–drug interactions with a high duration of action and no cytotoxicity (on HepG2 cells). We believe that, all these excellent assets make from compound **6f** a good candidate for a future drug.

Future perspective

Considering the high versatility and aggressively of *Mtb* bacillus, the great and urgent demand of pharmaceutical industry, as well as enormous amount of effort for discovery of new anti-TB entities, we believe that substantially improvements in drug discovery of new antitubercular agents will be performed in the next decade. A special attention will be paid further to pyridine and imidazole scaffolds, which have an enormous potential of growth.

Summary points
• Design, synthesis and antimycobacterial activity of two new classes of *bis*-(imidazole/benzimidazole)-pyridine derivatives.
• The reaction pathway is advantageous and straight applicable and, the newly 15 synthesized compounds was subject to antimycobacterial assay.
• Interesting structure–activity relationship correlations have been done. Anchoring of a *p-chloro*-benzoyl moiety in the 3-position of imidazole/benzimidazole moiety is favorable for activity.
• The anti-TB assay reveal that our compounds possess an excellent solubility in microbiological medium, have an excellent anti-TB activity against both replicating and nonreplicating Mtb, are not cytotoxic, exhibited a very good intracellular activity and are active against drug-resistant Mtb strains, some compounds have a bactericidal mechanism.
• The pharmacokinetic absorption, distribution, metabolism, excretion and toxicity screening performed for one compound, indicating a lower clearance rate, a great half-time *in vivo*, a low potential for drug–drug interactions with a high duration of action and no cytotoxicity. We believe that, all these excellent assets make from this compound a good candidate for a future drug.

Supplementary data

Supplementary data related to this article can be found in the online version, and contain NMR spectra of compound **6e** and all protocols related to the antimycobacterial evaluation of tested compounds. To view the supplementary data that accompany this paper please visit the journal website at: www.future-science/doi/suppl/10.4155/fmc-2019-0063

References

Papers of special note have been highlighted as: ● of interest; ●● of considerable interest

1. WHO, Global tuberculosis report (2017). www.who.int/tb/publications/global_report/en/

2. Sacks LV, Behrman RE. Developing new drugs for the treatment of drug-resistant tuberculosis: a regulatory perspective. *Tuberculosis* 88(Suppl. 1), S93–S100 (2008).

3. Nguyen L, Pieters J. Mycobacterial subversion of chemotherapeutic reagents and host defense tactics: challenges in tuberculosis drug development. *Annu. Rev. Pharmacol. Toxicol.* 49, 427–453 (2009).

4. Burman WJ, Jones BE. Treatment of HIV-related tuberculosis in the era of effective antiretroviral therapy. *Am. J. Respir. Crit. Care Med.* 164(1), 7–12 (2001).

●● **An informative article containing recommendations for the use of antiretroviral therapy among patients with HIV-related tuberculosis (TB).**

5. Lawn SD, Zumla AI. Tuberculosis. *Lancet* 378(9785), 57–72 (2011).

6. Kakkar AK, Dahiya N. *Bedaquiline* for the treatment of resistant tuberculosis: promises and pitfalls. *Tuberculosis* 94(4), 357–362 (2014).

7. Gler MT, Skripconoka V, Sanchez-Garavito E *et al. Delamanid* for multidrug-resistant pulmonary tuberculosis. *N. Engl. J. Med.* 366(23), 2151–2160 (2012).

● **The results of the presented study suggest that *Delamanid*, a nitro-dihydro-imidazooxazole derivative, could enhance treatment options for multidrug-resistant TB.**

8. Beena RDS. Antituberculosis drug research: a critical overview. *Med. Res. Rev.* 33(4), 693–693 (2013).

●● **A review article outlines various classes of compounds (such as quinolines, diamines, quinolones, pyrimidines and purines) as future drug candidates for anti-TB.**

9. Dover LG, Coxon GD. Status and research strategies in tuberculosis drug development. *J. Med. Chem.* 54(18), 6157–6165 (2011).

10. Ma Z, Lienhardt C, McLleron H *et al.* Global tuberculosis drug development pipeline: the need and the reality. *Lancet* 375(9731), 2100–2109 (2010).

11. Zhang Y, Post-Martens K, Denkin S. New drug candidates and therapeutic targets for tuberculosis therapy. *Drug Discov. Today* 11(1–2), 21–27 (2006).

12. Keri RS, Rajappa CK, Patil SA *et al.* Benzimidazole-core as an antimycobacterial agent. *Pharmacol. Rep.* 68(6), 1254–1265 (2016).

●● **A review article details the recent advancements on benzimidazole derivatives for anti-TB applications.**

13. Akhtar W, Khan MF, Verma G *et al.* Therapeutic evolution of benzimidazole derivatives in the last quinquennial period. *Eur. J. Med. Chem.* 126, 705–753 (2017).

14. Jeon AB, Ackart DF, Li W *et al.* 2-Aminoimidazoles collapse mycobacterial proton motive force and block the electron transport chain. *Sci. Rep.* 9, 1513 (2019).

15. Lu X, Williams Z, Hards K *et al.* Pyrazolo[1,5- a]pyridine inhibitor of the respiratory cytochrome bcc complex for the treatment of drug-resistant tuberculosis. *ACS Infect. Dis.* 5(2), 239–249 (2019).

16. Fan YL, Jin XH, Huang ZP *et al.* Recent advances of imidazole-containing derivatives as anti tubercular agents. *Eur. J. Med. Chem.* 150, 347–365 (2018).

17. Campaniço A, Moreira R, Lopes F. Drug discovery in tuberculosis. New drug targets and antimycobacterial agents. *Eur. J. Med. Chem.* 150, 525–545 (2018).

18. Al Matarneh CM, Ciobanu, Apostu M, Mangalagiu II, Danac R. Cycloaddition versus amidation in reactions of 2-amino-2-oxoethyl-phenanthrolinium ylides to activated alkynes and alkenes. *CR Chim.* 21(1), 1–8 (2018).

19. Olaru A, Vasilache V, Danac R *et al.* Antimycobacterial activity of nitrogen heterocycles derivatives: 7-(pyridine-4-yl)-indolizine derivatives. Part VII. *J. Enzyme Inhib. Med. Chem.* 32(1), 1291–1298 (2017).

•   **Describes the synthesis of some indolizinyl-pyridinium quaternary salts and the evaluation of antimicrobial activity against *Mycobacterium tuberculosis*.**

20. Mantu D, Antoci V, Nicolescu A *et al.* Synthesis, stereochemical studies and antimycobacterial activity of new acetylhydrazines pyridazinone. *Curr. Org. Synth.* 14(1), 112–119 (2017).

21. Al Matarneh CM, Ciobanu CI, Mangalagiu II *et al.* Design, synthesis and antimycobacterial evaluation of some new azaheterocycles with 4,7-phenanthroline skeleton. Part VI. *J. Serb. Chem. Soc.* 81(2), 133–140 (2016).

22. Mantu D, Antoci V, Moldoveanu C *et al.* Hybrid imidazole (benzimidazole)/pyridine (quinoline) derivatives and evaluation of their anticancer and antimycobacterial activity. *J. Enzyme Inhib. Med. Chem.* 31(Suppl. 2), 96–103 (2016).

•   **Describes the synthesis, structure and *in vitro* anticancer and antimycobacterial activity of new hybrid imidazol(benzimidazol)/2-aminopyridine(8-aminoquinoline) derivatives.**

23. Al Matarneh CM, Mangalagiu II, Shova S *et al.* Synthesis, structure, antimycobacterial and anticancer evaluation of new pyrrolo-phenanthroline derivatives. *J. Enzyme Inhib. Med. Chem.* 31(3), 470–480 (2016).

24. Danac R, Al Matarneh CM, Shova S *et al.* New indolizines with phenanthroline skeleton: synthesis, structure, antimycobacterial and anticancer evaluation. *Bioorg. Med. Chem.* 23(10), 2318–2327 (2015).

25. Danac R, Daniloaia T, Antoci V *et al.* Design, synthesis and antimycobacterial activity of some new azaheterocycles: phenanthroline with *p-halo*-benzoyl skeleton. Part V. *Lett. Drug Des. Discov.* 12(1), 14–17 (2015).

26. Danac R, Mangalagiu II. Antimycobacterial activity of nitrogen heterocycles derivatives: bipyridine derivatives. Part III. *Eur. J. Med. Chem.* 74, 664–670 (2014).

27. Mantu D, Antoci V, Mangalagiu II. Design, synthesis and antituberculosis activity of some new pyridazine derivatives: bis-pyridazine. Part IV. *Infect. Dis. Drug Targets* 13(5), 344–351 (2013).

28. Mantu D, Luca C, Moldoveanu C *et al.* Synthesis and antituberculosis activity of some new pyridazine derivatives. Part II. *Eur. J. Med. Chem.* 45(11), 5164–5168 (2010).

29. Moldoveanu C, Mangalagiu G, Drochioiu G *et al.* New antituberculosis compounds derived from diazine. *An. Stiint. Univ. "Al.I. Cuza" Iasi* 11, 367–374 (2003)

30. Lungu CN, Bratanovici BI, Grigore MM *et al.* Hybrid imidazole-pyridine derivatives: an approach to novel anticancer DNA intercalators. *Curr. Med. Chem.* (2018) (Epub ahead of print).

•   **Investigates the antimicrobial and antitumoral properties of some imidazole-pyridine derivatives by experimental and computational methods.**

31. Haque RA, Asekunowo PO, Razali MR. Dinuclear silver(I)-N-heterocyclic carbene complexes of N-allyl substituted (benz)imidazol-2-ylidenes with pyridine spacers: synthesis, crystal structures, nuclease and antibacterial studies. *Transition Met. Chem.* 39(3), 281–290 (2014).

32. Bevan CD, Lloyd RS. A high-throughput screening method for the determination of aqueous drug solubility using laser nephelometry in microtiter plates. *Anal. Chem.* 72(8), 1781–1787 (2000).

33. Castagnolo D, De Logu A, Radi M *et al.* Synthesis, biological evaluation and SAR study of novel pyrazole analogues as inhibitors of *Mycobacterium tuberculosis*. *Bioorg. Med. Chem.* 16(18), 8587–8591 (2008).

34. Ollinger J, Bailey MA, Moraski GC *et al.* A dual read-out assay to evaluate the potency of compounds active against *Mycobacterium tuberculosis*. *PLoS ONE* 8(4), e60531 (2013).

35. Zelmer A, Carroll P, Andreu N *et al.* A new *in vivo* model to test anti-tuberculosis drugs using fluorescent imaging. *J. Antimicrob. Chemother.* 67(8), 1948–1960 (2012).

36. Carroll P, Schreuder LJ, Muwanguzi-Karugaba J *et al.* Sensitive detection of gene expression in mycobacteria under replicating and non-replicating conditions using optimized far-red reporters. *PLoS ONE* 5(3), e9823 (2010).

37. Lambert RJ, Pearson J. Susceptibility testing: accurate and reproducible minimum inhibitory concentration (MIC) and non-inhibitory concentration (NIC) values. *J. Appl Microbiol.* 88(5), 784–790 (2000).

38. Kuti JL. Optimizing antimicrobial pharmacodynamics: a guide for stewardship program. *Rev. Med. Clin. Condes.* 27(5), 615–624 (2016).

39. Cho SH, Warit S, Wan B *et al.* Low-oxygen-recovery assay for high-throughput screening of compounds against nonreplicating *Mycobacterium tuberculosis*. *Antimicrob. Ag. Chemother.* 51(4), 1380–1385 (2007).

40. Andreu N, Zelmer A, Fletcher T *et al.* Optimisation of bioluminescent reporters for use with mycobacteria. *PLoS ONE* 5(5), e10777 (2010).

41.   Wayne LG. *In vitro* model of hypoxically induced nonreplicating persistence of *Mycobacterium tuberculosis*. In: *Mycobacterium Tuberculosis Protocols*. Parish T, Stoker NG (Eds.). Humana Press, NJ, USA, 247–270 (2001).

42.   Franzblau SG, Witzig RS, McLaughlin JC *et al.* Rapid, low-technology MIC determination with clinical *Mycobacterium tuberculosis* isolates by using the microplate Alamar Blue Assay. *J. Clin. Microbiol.* 36(2), 362–366 (1998).

43.   Banker MJ, Clark TH, Williams JA. Development and validation of a 96-well equilibrium dialysis apparatus for measuring plasma protein binding. *J. Pharm. Sci.* 92(5), 967–974 (2003).

44.   Smith DA, Di L, Kerns EH. The effect of plasma protein binding on *in vivo* efficacy: misconceptions in drug discovery. *Nat. Rev. Drug. Discov.* 9(12), 929–939 (2010).

45.   Stewart BH, Chan OH, Lu RH *et al.* Comparison of intestinal permeabilities determined in multiple *in vitro* and *in situ* models: relationship to absorption in humans. *Pharm. Res.* 12(5), 693–699 (1995).

46.   Artursson P, Palm K, Luthman K. Caco-2 monolayers in experimental and theoretical predictions of drug transport. *Adv. Drug Deliv. Rev.* 46(1–3), 27–43 (2001).

47.   Yee S. *In vitro* permeability across Caco-2 cells (colonic) can predict *in vivo* (small intestinal) absorption in man – fact or myth. *Pharm. Res.* 14(6), 763–766 (1997).

48.   Endres CJ, Hsiao P, Chung FS *et al.* The role of transporters in drug interactions. *Eur. J. Pharm. Sci.* 27(5), 501–517 (2006).

49.   Balimane PV, Han YH, Chong S. Current industrial practices of assessing permeability and P-glycoprotein interaction. *AAPS J.* 8(1), E1–E13 (2006).

50.   Walsky RL, Obach RS. Validated assays for human cytochrome P450 activities. *Drug Metab. Dispos.* 32(6), 647–660 (2004).

51.   Kim MJ, Kim H, Cha IJ *et al.* High-throughput screening of inhibitory potential of nine cytochrome P450 enzymes *in vitro* using liquid chromatography/tandem mass spectrometry. *Rapid Commun. Mass Spectrom.* 19(18), 2651–2658 (2005).

52.   Fowler S, Zhang H. *In vitro* evaluation of reversible and irreversible cytochrome P450 inhibition: current status on methodologies and their utility for predicting drug–drug interactions. *AAPS J.* 10(2), 410–424 (2008).

53.   Houston JB. Utility of *in vitro* drug metabolism data in predicting *in vivo* metabolic clearance. *Biochem. Pharmacol.* 47(9), 1469–1479 (1994).

54.   Obach RS. Prediction of human clearance of twenty-nine drugs from hepatic microsomal intrinsic clearance data: an examination of *in vitro* half-life approach and non-specific binding to microsomes. *Drug Metab. Dispos.* 27(11), 1350–1359 (1999).

55.   Di L, Kerns EH, Ma XJ *et al.* Applications of high throughput microsomal stability assay in drug discovery. *Comb. Chem. High Throughput Screen.* 11(6), 469–476 (2008).

56.   Crouch SP, Kozlowski R, Slater KJ *et al.* The use of ATP bioluminescence as a measure of cell proliferation and cytotoxicity. *J. Immunol. Methods* 160(1), 81–88 (1993).

57.   Lundin A, Hasenson M, Persson J *et al.* Estimation of biomass in growing cell lines by ATP assay. *Methods Enzymol.* 133, 27–42 (1986).

58.   Maehara Y, Anai H, Tamada R *et al.* The ATP assay is more sensitive than the succinate dehydrogenase inhibition test for predicting cell viability. *Eur. J. Cancer Clin. Oncol.* 23(3), 273–276 (1987).

59.   Slater K. Cytotoxicity tests for high-throughput drug discovery. *Curr. Opin. Biotechnol.* 12(1), 70–74 (2001).